Estimation of Phonon Mean Free Path in Small-Scaled Si Wire by Monte Carlo Simulation

Yuhei Suzuki
Faculty of Information Science and Technology
Osaka Institute of Technology
Osaka, Japan
yuhei.suzuki@rsh.oit.ac.jp

Yuma Fujita
Faculty of Information Science and Technology
Osaka Institute of Technology
Osaka, Japan
e1q17075@st.oit.ac.jp

Khotimatul Fauziah
Research Institute of Electronics
Shizuoka University
Shizuoka, Japan
khotimatul.fauziah@gmail.com

Takuto Nogita
Research Institute of Electronics
Shizuoka University
Shizuoka, Japan
nogita.taketo.15@shizuoka.ac.jp

Hiroya Ikeda
Research Institute of Electronics
Shizuoka University
Shizuoka, Japan
ikeda.hiroya@shizuoka.ac.jp

Takanobu Watanabe
Graduate School of Engineering
Waseda University
Tokyo, Japan
watanabe-t@waseda.jp

Yoshinari Kamakura
Faculty of Information Science and Technology
Osaka Institute of Technology
Osaka, Japan
yoshinari.kamakura@oit.ac.jp

***Abstract*—A phonon transport in Si wire structures were simulated based on a Monte Carlo method to clarify the influence of the wire geometry and the surface roughness on thermal conductivity and the phonon-drag component of Seebeck coefficient. The mean free path (MFP) spectrum was estimated by tracing the simulated phonons. The MFPs of 1 THz phonons which mainly contribute to Seebeck coefficient become shorter with a decrease of the wire width for rough surfaces. This agrees with experimental observation of Seebeck coefficient. The MFPs of 3 THz phonons which mainly contribute to thermal conductivity were influenced even by small-roughness surfaces.**

***Index Terms*—Si, phonon, Monte Carlo simulation**

I. Introduction

In recent years, thermoelectric devices attract much attention as one of the applications of nanostructured Si CMOS process technology [1]. Since the conversion efficiency monotonically increases with the figure of merit $ZT(\propto \sigma S^2/\kappa$, where σ, S, and κ are the electrical conductivity, the Seebeck coefficient, and the thermal conductivity, respectively), the efficient thermoelectric devices require the higher σ and S, and the lower κ. Especially, the nanostructures, such as nanowires [2], [3], and nano-porous structure [4], are greatly expected to enhance ZT by decreasing κ. On the other hand, the decrease of S has been experimentally observed in narrow Si wires with the width of < 1 μm [5], [6], whose mechanism has been supposed to be due to the vanishment of the phonon drag contribution to S [7]. However, the detailed mechanisms have not been clarified yet, and the theoretical analyses are needed.

So, in this study, we carry out a phonon transport simulation in Si wire structures based on a Monte Carlo (MC) method to solve the phonon's Boltzmann transport equation [8]. Then, the effect of the wire geometry and the surface roughness on κ and the phonon-drag component of S ($S_{\rm pd}$) is discussed in terms of the phonon mean free path (MFP) spectrum.

II. Simulation Method

The phonon density of states(DOS) and the group velocity averaged over constant-energy surfaces were calculated from the realistic dispersion relation (Fig. 1) [8]. For the phonon scattering models, the phonon-phonon, the phonon-impurity, and the phonon-boundary scattering processes were taken into account. The formula given in [9] was adopted for the Umklapp phonon scattering processes, but the parameters were readjusted to reproduce the measured bulk κ (Fig. 2) [10]. For phonon-impurity scattering processes, the formula is given in [11] which considers the difference in the mass, the radius, and the compressibility between Si and P atoms. The parameters for the phonon-impurity scattering were also readjusted to reproduce the measured bulk κ (Fig. 3) [12]–[16].

The specularity of crystal boundary p was employed to calculate the phonon-boundary scattering processes given in the following formula [17]:

$$p = \exp(-16\pi^2\eta^2\cos^2(\theta)/\lambda^2), \tag{1}$$

where η is the root-mean-square (RMS) roughness of crystal surface, λ is the phonon wave length, θ is the incident angle of phonons onto the surface.

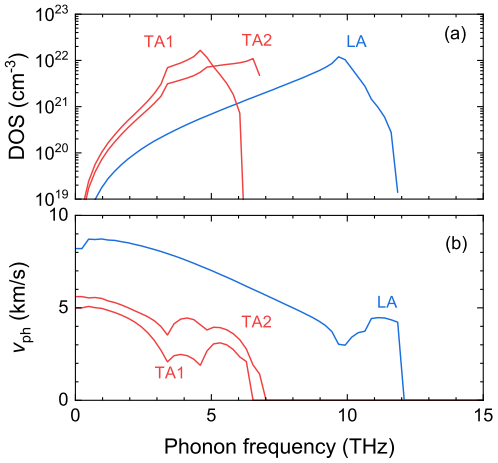

Fig. 1: Phonon frequency dependence of (a) density of states and (b) group velocity (v_{ph}) of transverse acoustic (TA1, TA2) and longitudinal acoustic (LA) phonons calculated from the approximated dispersion curves [8].

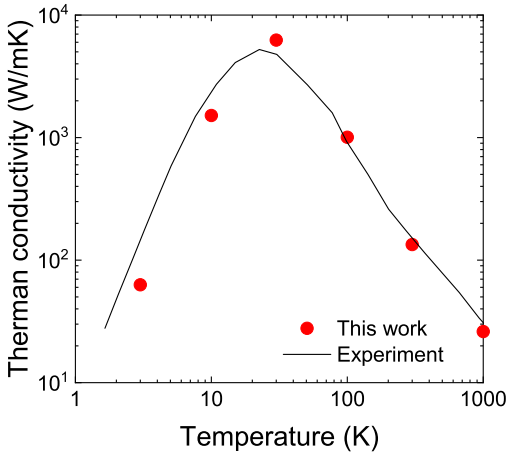

Fig. 2: Comparison of temperature-dependency of thermal conductivity of bulk Si between the simulation (dots) and experiment (line) [10].

III. Simulation Results and Discussion

Figure 4 shows an example of a simulated phonon trajectory in a typical structure of Si wire together with Si contact pads which were formed on an silicon-on-insulator (SOI) layer. In this work, to reduce the computational time, we simulated the phonon transport only in the Si wire region as shown in Fig. 5. The wire thickness was assumed to be 30 nm. The RMS roughness at the top and the bottom surfaces were fixed to 0.2 nm, while the sidewall roughness η_{side} was varied from 0.2 to 2.0 nm. The doping (P) concentration was set to 10^{19} cm^{-3}, which is normally used to achieve higher ZT with Si [18].

Figure 6 shows the simulated phonon trajectories in the Si

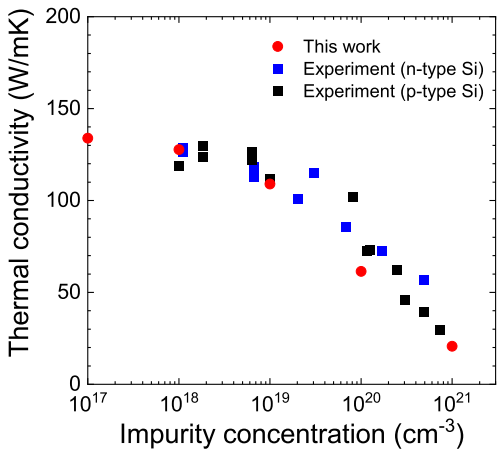

Fig. 3: Comparison of impurity concentration-dependency on thermal conductivity of bulk Si between the simulation (red) and experiment for n-type (blue) and p-type (black) [12]–[16].

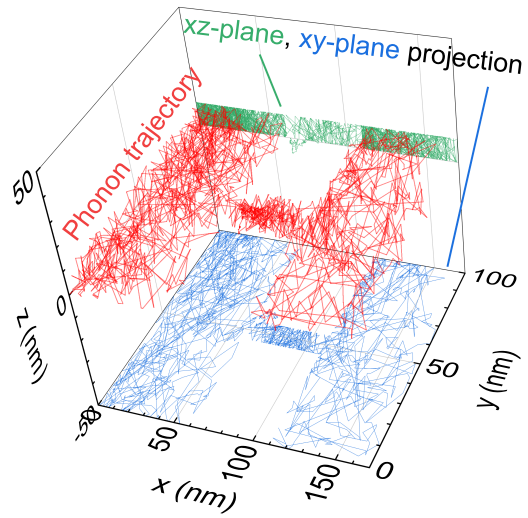

Fig. 4: Phonon trajectory in an actual Si wire structure with Si pads formed in SOI substrate.

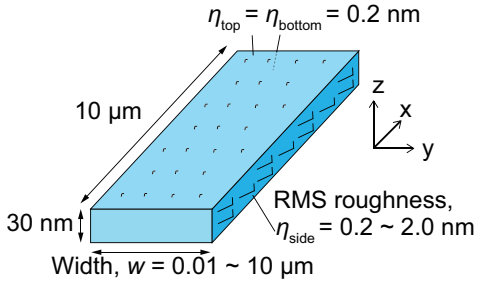

Fig. 5: Schematic of test device structure to simulate phonon mean free path.

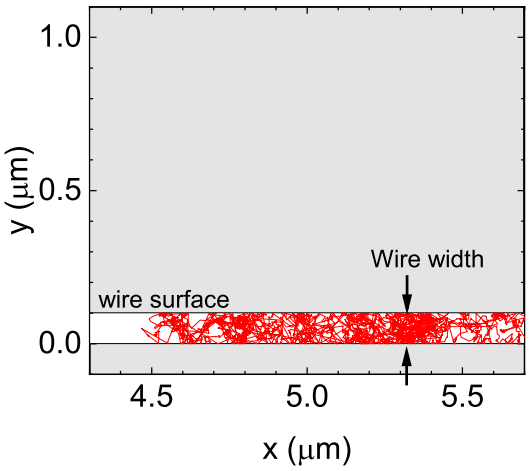

(a) W = 0.1 μm

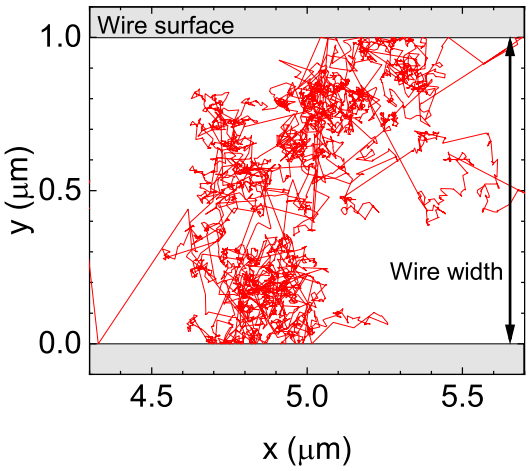

(b) W = 1 μm

Fig. 6: Phonon trajectories in the device structure shown in Fig. 5 for the width of (a) 0.1 μm and (b) 1 μm. η_{side} is 1.4 nm.

wires with the wire width W of 0.1 and 1 μm at the $\eta_{\mathrm{side}} = 1.4$ nm. Phonons in the case of $W = 0.1$ μm reach the surfaces of the sidewalls per unit time more frequently than the case of W = 1 μm, that is, the probability of the phonon-boundary scattering in a narrow-wire structure is higher.

The phonon MFP spectrum were estimated by tracing the phonon trajectrories during the simulation as plotted in Fig. 7. The spectrum of the phonon MFP is affected by the shape of DOS shown in Fig. 1 (a). At the phonon frequencies from 2 to 5 THz, the MFPs of the Si wires are shorter than that of the bulk Si and become progressively lower with decreasing the Si wire width. In contrast, at the low phonon frequencies, the MFPs of wide Si wires ($W \geq 1$ μm) are closed to the MFPs of the bulk Si. In Fig. 8, the phonon MFPs as a function of W for the phonon frequencies of 1 THz and 3 THz are shown. As

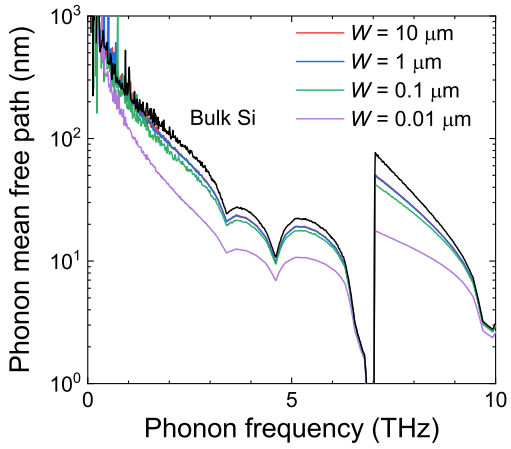

Fig. 7: Phonon mean free path for Si wire and bulk Si with respect to phonon frequency. η_{side} is 1.4 nm.

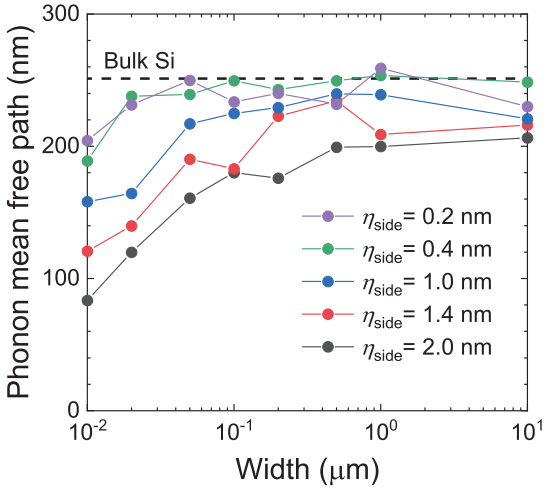

(a) f = 1 THz

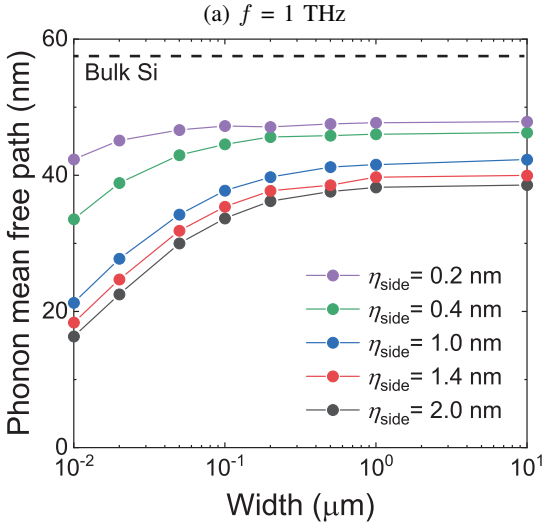

(b) f = 3 THz

Fig. 8: Comparison of phonon mean free path among RMS roughness with respect to wire width for phonon frequencies f of (a) 1 THz and (b) 3 THz.

suggested in [7], $S_{\rm pd}$ and κ at 300 K are mainly contributed by the different frequency phonons with $\sim$ 1 THz and $\sim$ 3 THz, respectively. The MFPs of 1 THz phonons are dependent on $\eta_{\rm side}$ and become shorter with decreasing W below 1 μm for $\eta_{\rm side} \geq$ 1.0 nm, because the low-frequency, i.e., long-λ, phonons are specularly reflected at the boundaries especially with smaller η as shown in Eq. (1).

In the experiment of [6], the $\eta_{\rm side}$ is estimated to be $>\sim$ 1.0 nm. The result shown in Fig. 8a indicates that $S_{\rm pd}$ ($\propto$ MFP [19]) decreases with W ($<$ 1 μm) for large $\eta_{\rm side}$, which is consistent with the observation in [6]. On the other hand, the MFPs of 3 THz phonons also dependent on $\eta_{\rm side}$ and converge on $\sim$ 48 nm at $\eta_{\rm side}$ = 0.2 nm, but are not asymptotic to that of bulk Si (Fig. 8b). The reduction of the MFPs at 3 THz phonons from the bulk Si is caused by the phonon-boundary scattering at the top and bottom surface even though they are smooth as $\eta_{\rm top} = \eta_{\rm bottom} = 0.2$ nm. Furthermore, it is suggested that if the smaller $\eta_{\rm side}$ could be achieved, then the decrease of κ is expected without the penalty of the decrease of $S_{\rm pd}$, which is desirable for ZT.

IV. Conclusions

The simulation using a MC method for a nanoscaled Si wire to estimate the phonon MFP has been carried out. The dependency of simulated phonon MFP on the wire width was consistent with the experimental result. The Si wire with smooth surface roughness is expected to enhance the conversion efficiency due to a preserved $S_{\rm pd}$ and a decrease in κ.

Acknowledgment

This work was supported by JST-CREST under Grant JPMJCR19Q5.

References

[1] M. Tomita, S. Oba, Y. Himeda, R. Yamato, K. Shima, T. Kumada, M. Xu, H. Takezawa, K. Mesaki, K. Tsuda *et al.*, "Modeling, simulation, fabrication, and characterization of a 10-μw/cm^2 class si-nanowire thermoelectric generator for iot applications," *IEEE Transactions on Electron Devices*, vol. 65, no. 11, pp. 5180–5188, 2018.

[2] A. I. Boukai, Y. Bunimovich, J. Tahir-Kheli, J. K. Yu, W. A. Goddard, and J. R. Heath, "Silicon nanowires as efficient thermoelectric materials," *Nature*, vol. 451, no. 7175, pp. 168–171, 2008.

[3] A. I. Hochbaum, R. Chen, R. D. Delgado, W. Liang, E. C. Garnett, M. Najarian, A. Majumdar, and P. Yang, "Enhanced thermoelectric performance of rough silicon nanowires," *Nature*, vol. 451, no. 7175, pp. 163–167, 2008.

[4] R. Anufriev and M. Nomura, "Reduction of thermal conductance by coherent phonon scattering in two-dimensional phononic crystals of different lattice types," *Physical Review B*, vol. 93, no. 4, p. 045410, 2016.

[5] F. Salleh, T. Oda, Y. Suzuki, Y. Kamakura, and H. Ikeda, "Phonon drag effect on seebeck coefficient of ultrathin p-doped si-on-insulator layers," *Applied Physics Letters*, vol. 105, no. 10, p. 102104, 2014.

[6] K. Fauziah, Y. Suzuki, Y. Narita, Y. Kamakura, T. Watanabe, F. Salleh, and H. Ikeda, "Effect of phonon-drag contributed seebeck coefficient on si-wire thermopile voltage output," *IEICE Transactions on Electronics*, vol. 102, no. 6, pp. 475–478, 2019.

[7] J. Zhou, B. Liao, B. Qiu, S. Huberman, K. Esfarjani, M. S. Dresselhaus, and G. Chen, "Ab initio optimization of phonon drag effect for lower-temperature thermoelectric energy conversion," *Proceedings of the National Academy of Sciences*, vol. 112, no. 48, pp. 14 777–14 782, 2015.

[8] K. Kukita and Y. Kamakura, "Monte carlo simulation of phonon transport in silicon including a realistic dispersion relation," *Journal of Applied Physics*, vol. 114, no. 15, p. 154312, 2013.

[9] P. Chantrenne, J. Barrat, X. Blase, and J. Gale, "An analytical model for the thermal conductivity of silicon nanostructures," *Journal of applied physics*, vol. 97, no. 10, p. 104318, 2005.

[10] M. Holland, "Analysis of lattice thermal conductivity," *Physical review*, vol. 132, no. 6, p. 2461, 1963.

[11] P. Klemens, "The scattering of low-frequency lattice waves by static imperfections," *Proceedings of the Physical Society. Section A*, vol. 68, no. 12, p. 1113, 1955.

[12] G. A. Slack, "Thermal conductivity of pure and impure silicon, silicon carbide, and diamond," *Journal of Applied physics*, vol. 35, no. 12, pp. 3460–3466, 1964.

[13] Y. Lee and G. S. Hwang, "Mechanism of thermal conductivity suppression in doped silicon studied with nonequilibrium molecular dynamics," *Physical Review B*, vol. 86, no. 7, p. 075202, 2012.

[14] M. Asheghi, K. Kurabayashi, R. Kasnavi, and K. Goodson, "Thermal conduction in doped single-crystal silicon films," *Journal of applied physics*, vol. 91, no. 8, pp. 5079–5088, 2002.

[15] A. Stranz, J. Kähler, A. Waag, and E. Peiner, "Thermoelectric properties of high-doped silicon from room temperature to 900 k," *Journal of electronic materials*, vol. 42, no. 7, pp. 2381–2387, 2013.

[16] Y. Ohishi, J. Xie, Y. Miyazaki, Y. Aikebaier, H. Muta, K. Kurosaki, S. Yamanaka, N. Uchida, and T. Tada, "Thermoelectric properties of heavily boron-and phosphorus-doped silicon," *Japanese Journal of Applied Physics*, vol. 54, no. 7, p. 071301, 2015.

[17] J. M. Ziman, *Electrons and phonons: the theory of transport phenomena in solids*. Oxford university press, 2001.

[18] M. H. Elsheikh, D. A. Shnawah, M. F. M. Sabri, S. B. M. Said, M. H. Hassan, M. B. A. Bashir, and M. Mohamad, "A review on thermoelectric renewable energy: Principle parameters that affect their performance," *Renewable and sustainable energy reviews*, vol. 30, pp. 337–355, 2014.

[19] E. Behnen, "Quantitative examination of the thermoelectric power of n-type si in the phonon drag regime," *Journal of applied physics*, vol. 67, no. 1, pp. 287–292, 1990.